pISSN 2384-1095
eISSN 2384-1109

iMRI 2019;23:17-25

https://doi.org/10.13104/imri.2019.23.1.17

iMRI
Investigative Magnetic Resonance Imaging

Diagnostic Significance of pH-Responsive Gd^{3+}-Based T_1 MR Contrast Agents

Sankarprasad Bhuniya[1,2], **Kwan Soo Hong**[1,3]

[1]Bioimaging Research Team, Korea Basic Science Institute, Cheongju, Korea
[2]Amrita Centre for Industrial Research & Innovation, Amrita Vishwa Vidyapeetham, Ettimadai, Coimbatore, India
[3]Graduate School of Analytical Science and Technology, Chungnam National University, Daejeon, Korea

Review Article

Received: August 10, 2018
Revised: January 30, 2019
Accepted: February 1, 2019

Correspondence to:
Kwan Soo Hong, Ph.D.
Bioimaging Research Team,
Korea Basic Science Institute,
161, Yeongudanji-ro, Ochang-eup, Cheongwon-gu, Cheongju 28119, Korea.
Tel. +82-43-240-5100
Fax. +82-43-240-5059
E-mail: kshong@kbsi.re.kr

We discuss recent advances in Gd-based T_1-weighted MR contrast agents for the mapping of cellular pH. The pH plays a critical role in various biological processes. During the past two decades, several MR contrast agents of strategic importance for pH-mapping have been developed. Some of these agents shed light on the pH fluctuation in the tumor microenvironment. A pH-responsive self-assembled contrast agent facilitates the visualization of tumor size as small as 3 mm^3. Optimization of various parameters is crucial for the development of pH-responsive contrast agents. In due course, the new contrast agents may provide significant insight into pH fluctuations in the human body.

Keywords: MR contrast agent; pH-mapping; T_1-W MRI

INTRODUCTION

Proton (H^+) is the smallest cationic species. It plays a crucial role in various biological events such as cell proliferation, apoptosis, enzymatic activity, protein degradation, and many other phenomena (1, 2). The H^+/pH concentrations are maintained within a narrow and restricted range (7.1-7.4) in the intracellular region by the membrane proton pump/proton transporter (3). The cytoplasmic pH sensor-regulator directly controls this process (4). Under normal physiological conditions, the protons flow from the extracellular environment to the intracellular region. However, the proton gradient in cancer cells occurs in the reverse direction to that in normal cells and away from cells to the extracellular regions. Anaerobic glycolysis in cancer generates lactic acid, which is transported to the extracellular region by carbonic anhydrase. Thus, the tumor extracellular environment is acidic (≤ 6.8). Such reverse proton gradient (Warburg effect) in cancer cells reduces the activity of cellular receptors and propagates a heterogenic tumor environment of hypoxia (5), which prevents the entry of chemotherapeutic agents to the tumor region. On the other hand, bacterial infections or pathogenic inflammation also creates an acidic environment (6, 7) due to macrophage infiltration (8). Virtually, the cellular acidosis represents abnormal and pathological status. Thus, various modalities have been used to map the pH fluctuation in living cells

with high spatiotemporal resolution. Different fluorescent probes have been strategically developed for mapping of extracellular and intracellular pH fluctuation under various artificial oxidative and reducing microenvironments (9-11). Also, several methods have been used to measure tissue pH via MRS and MRI modalities. Raghunand and his coworkers (12) used ^{31}P-NMR with 3-aminopropylphosphate (3-APP) to estimate intracellular pH in tissues. Mason et al. (13) reported the use of a fluorinated derivative of vitamin B6 as a pH-responsive ^{19}F-MRS agent, which readily enters the cells and regulates intra- and extra-cellular pH in rodent tumors. Ojugo et al. (14) also reported an ^{19}F-based strategy to measure extracellular pH. The inherent sensitivity of ^{1}H nuclei offers a unique strategy for pH mapping of tissues. Several workers have utilized the pH-sensitive proton resonance changes in imidazole and IEPA for pH measurement in breast and brain tumor tissues (15, 16). Vermathen et al. (17) successfully measured pH in brain tumor by ^{1}H-NMR after oral administration of histidine. A different approach was used for pH mapping in tissues using pH-sensitive proton-exchange agents (18). Ward and Balaban (19) introduced 5,6-dihydrouracil with multiple proton exchanges facilitating pH mapping based on self-calibrated pH data.

In the last decade, the major emphasis was placed on the development of pH-responsive T_1-weighted (W) Gd-based MR contrast agents. The Gd^{3+}-based contrast agent can be readily synthesized by incorporating a pH-responsive group in the DOTA/DTPA moiety, where the T_1 relaxivity fluctuated depending on the variation in the number of water molecules in the first coordination sphere of Gd^{3+}. Also, pH-dependent changes in Gd-based aggregation is another strategy designed for the development of pH-dependent T_1-W MR contrast agents.

In this review, we describe the critical features of Gd-based pH-responsive T_1-W MR contrast agents, the approaches for development of such contrast agents, and prospective applications in an animal model.

Gd^{3+}-Based T_1 MRI Contrast Agents and Relaxivity

Paramagnetic T_1 contrast agents positively influence MR images by changing the relaxation rate of water protons in the immediate vicinity of the contrast agent in the tissues. Such phenomenon was first demonstrated in the animal model using the Mn^{2+} complex (20). Since then, Gd^{3+} complexes have been used extensively as MR contrast agents for whole body imaging of humans. In 1988, a Gd-based MR contrast agent was used for the first time in clinical diagnosis. Since then, it has been routinely used as an invaluable component of MRI for disease diagnosis (21). Gd^{3+}-based contrast agents positively improve the longitudinal and transverse relaxation rates of the coordinated water proton. Nonetheless, the percentage of longitudinal relaxation of water proton is primarily enhanced to provide bright images. Commercially, cyclic and acyclic poly-aminocarboxylate derivatives are used as Gd^{3+} chelating agents for T_1-W MR imaging, in which single water molecules are coordinated to Gd^{3+} to generate sufficient proton relaxivity with high thermodynamic stability (Fig. 1). Currently available contrast agents are based on longitudinal relaxivity (r_1) of protons in the water molecules, which is directly coordinated with the Gd^{3+} ion in the first coordination sphere. The paramagnetic relaxation theory derived by Solomon-Bloembergen-Morgan (SBM) suggests (22-25) that proton relaxivity is proportional to the number of water molecule in the first coordination sphere, the fraction of bulk water in the secondary coordination sphere, and rapid water exchange rate (low water residence time to the metal ions) (Fig. 2). On the other hand, the proton relaxivity is inversely proportional to the tumbling motion. Under high contrast movement, the longitudinal relaxivity is low. For example, the longitudinal relaxivity (r_1) of one of the commercially available vascular contrast agents, Vasovist (MS-325), is increased 10-fold upon binding with the human serum albumin protein (26).

Recently, new paramagnetic contrast agents have been designed from inexpensive materials, e.g., polyamino-carboxylate, by optimizing the aforementioned parameters to obtain better relaxivity at higher magnetic fields (27). Most importantly, the new contrast agent yields significant data based on different analytes in the living system. The optimization of various relaxivity parameters in MR contrast agents for the estimation of pH fluctuation is critically described.

Design of pH-Responsive T_1 Contrast Agents and pH Sensing

As described, the pH-dependent changes in relaxivity of the contrast agent can be obtained by optimizing the relaxivity parameter. In 1999, Zhang and coworkers (28) developed a pH-responsive contrast agent using a tetra-carboxy amide-substituted cyclen combined with a non-coordinated phosphonate functionality ([Gd(1)]). It increased the relaxivity from pH 4 to 6. By contrast, the relaxivity decreased from pH 6 to 8.5. Such unusual behavior is attributed to the extensive H-bonding between

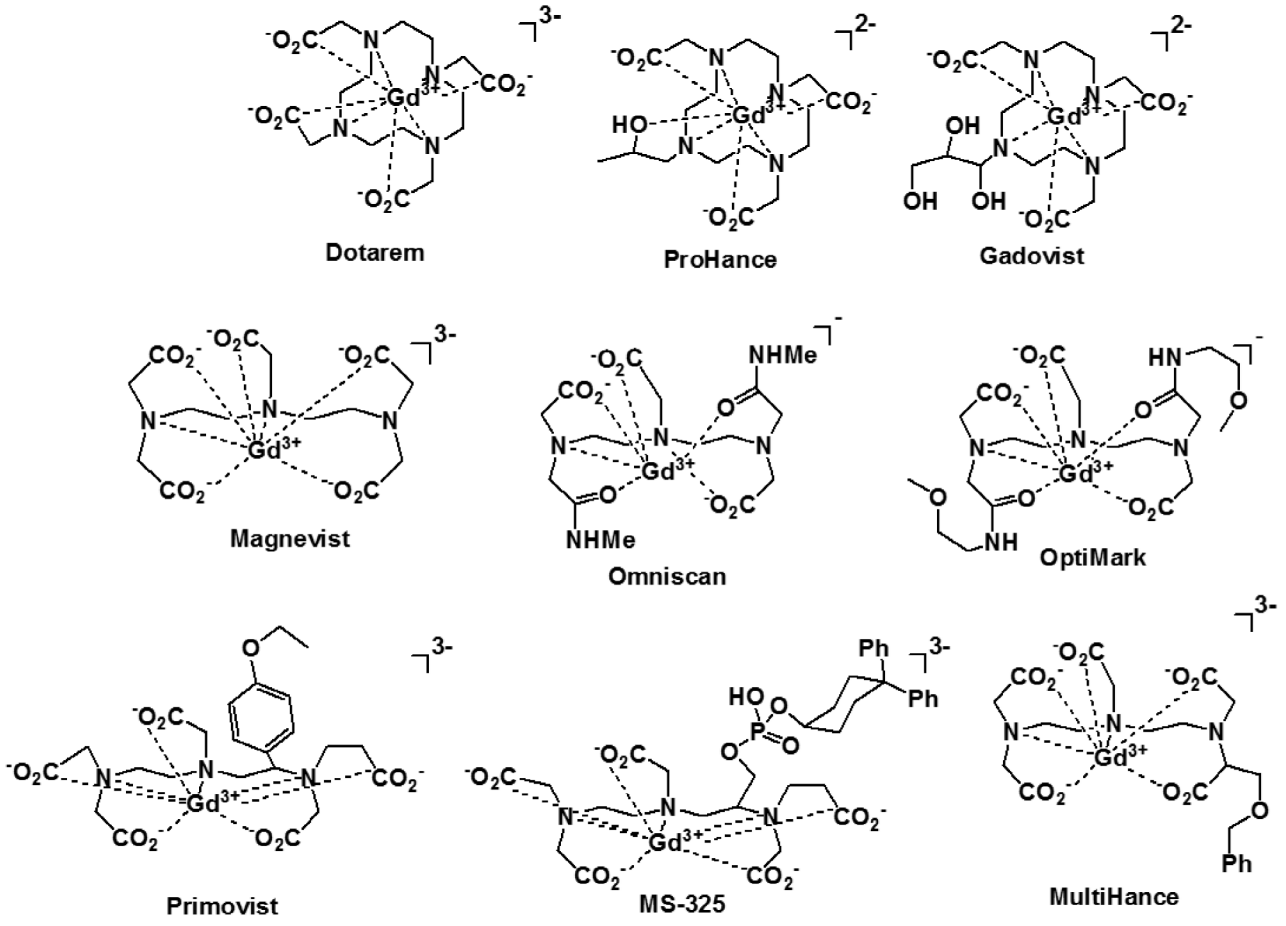

Fig. 1. Representative, clinically available, T_1-W Gd^{3+}-based contrast agents.

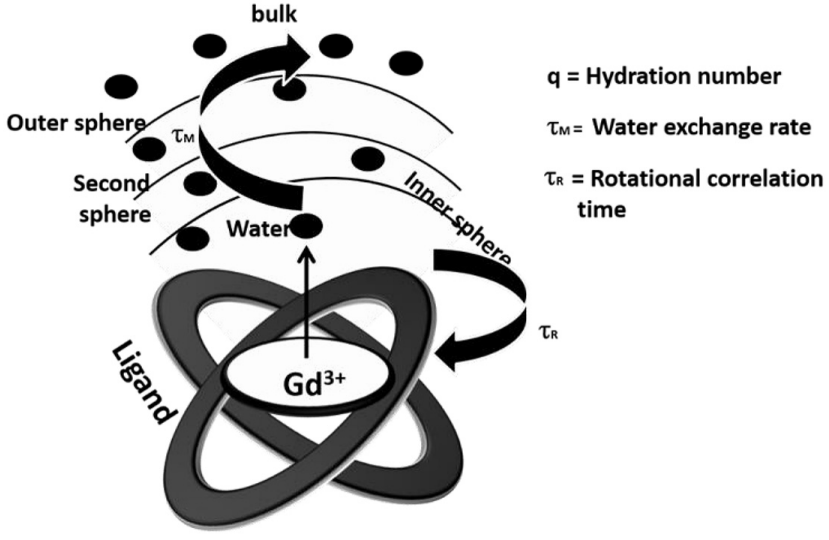

Fig. 2. Parameters controlling T_1 relaxivity (r_1).

the phosphonate moiety and the bulk water, which facilitated proton exchange between coordinated water and bulk water molecules, and enhanced the water-proton exchange rate. In 2008, the same group developed a dendrimer-based pH-responsive contrast agent [(Gd(11)] (29). The proton exchange rate between the bulk solvent and water molecules in the inner sphere and the second hydration spheres significantly altered the dendrimer contrast agent depending on the solvent pH. Ultimately, the T_1 relaxivity is significantly affected by the pH of the bulk solution. The pH of kidney and tumor was estimated *in vivo* using this contrast agent by comparing Δr_1 with the absolute r_1 value (30). The contrast agent was used in C6 glioma imaging using both high resolution pH_e (extracellular pH) mapping and TMI (time to maximal intensity). The pHe value varied within the heterogenic tumor environment and the overall pH was 6.87 ± 0.01 (± SE) (Fig. 3). To analyze the relationship between pHe and perfusion, the pH_e and TMI were compared pixel to pixel, showing robust correlation between pH_e and TMI throughout the tumor (R = 0.7).

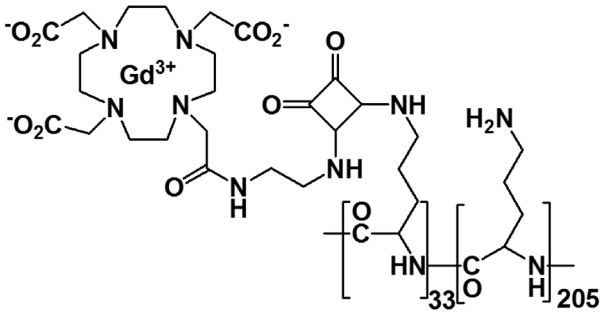

Fig. 4. Molecular structure of Gd-1 [$(Gd\text{-}DOTAam)_{33}\text{-}Orn_{205}$].

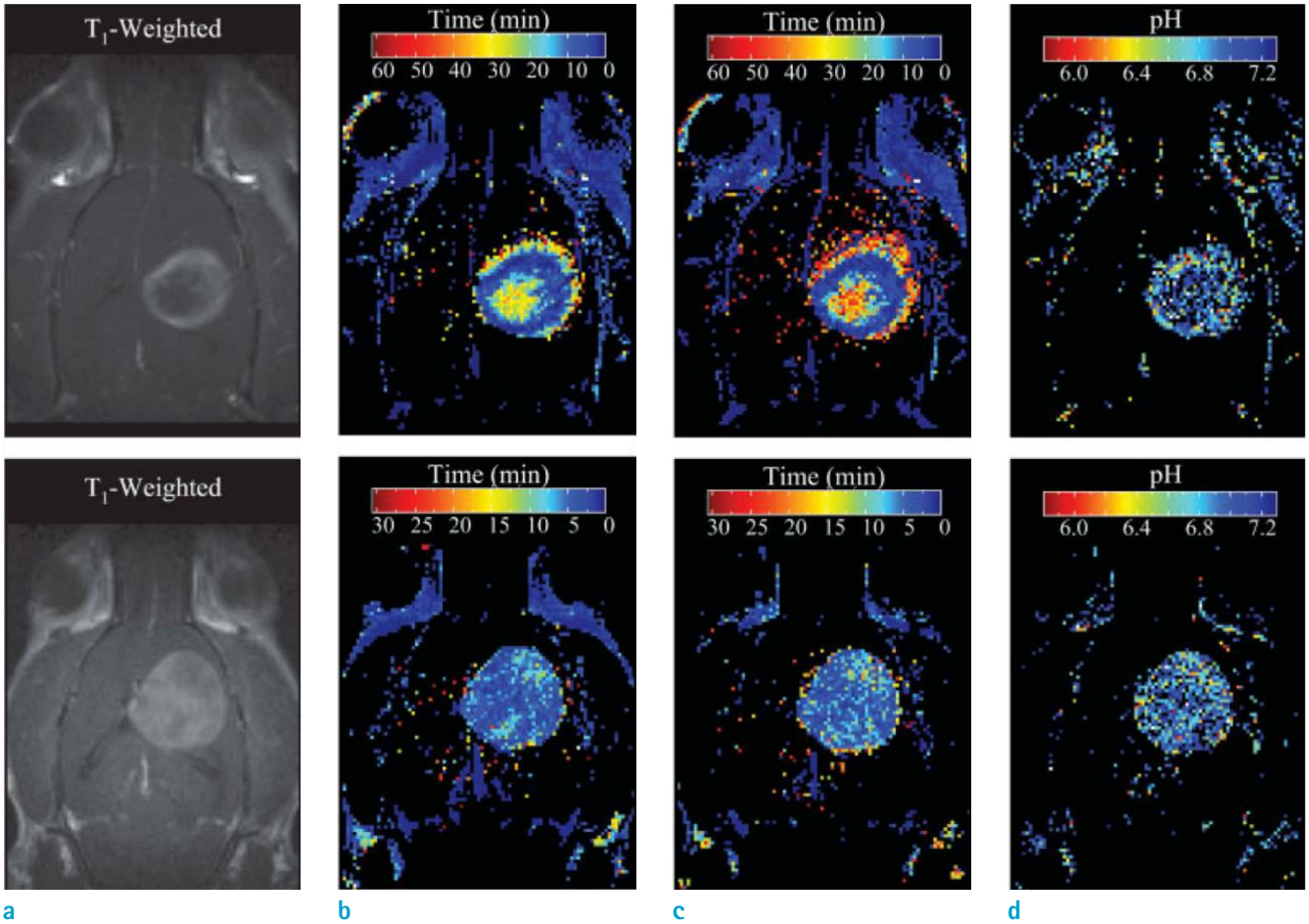

Fig. 3. Representative time to maximal intensity (TMI) and pHe maps in C6 gliomas *in vivo*. Upper and lower panels correspond to 2 different animals. (a) T_1-weighted images, (b) TMI maps of Gd-$DOTP^{5-}$, (c) TMI maps of Gd-DOTA-$4AmP^{5-}$, (d) pHe maps. Adapted from Garcia-Martin et al. (30) with permission of Wiley.

Aime and coworkers (31) have developed a Gd-complexed MRI T_1 contrast agent Gd-1 [(Gd-DOTAam)$_{33}$-Orn$_{205}$)] (Fig. 4), which showed R_2/R_1 changes depending on pH variation in the solution. The changes in ratiometric relaxivity at higher magnetic field were estimated at 600 MHz and 25°C. The ratiometric relaxivity ratio (R_2/R_1) increased gradually from pH 7 to pH 12 (Fig. 5). The R_2/R_1 relaxivity ratio of Gd-1 was independent of absolute concentrations of contrast agent; instead, the molecular tumbling motion, water exchange rate, and electronic relaxation were optimized to map pH fluctuation.

Toth and his group (32) developed fullerene-based Gd complexes Gd@$C_{60}(OH)_x$ and Gd@$C_{60}[C(COOH)_2]_{10}$ for T_1-WMR tracking of pH. As shown in Figure 6, the relaxivity (r_1) decreased gradually with increase in the pH. Dynamic light scattering (DLS) study was used to demonstrate the increased aggregation of both Gd@$C_{60}(OH)_x$ and Gd@$C_{60}[C(COOH)_2]_{10}$ at lower pH at hydrodynamic diameters of 700 nm and 1200 nm, respectively, at pH 4. By contrast, the diameter was reduced to 70 nm and 50 nm, respectively, at pH 9. The reduction in the hydrodynamic radius of Gd-fullerene at higher pH directly influenced the tumbling

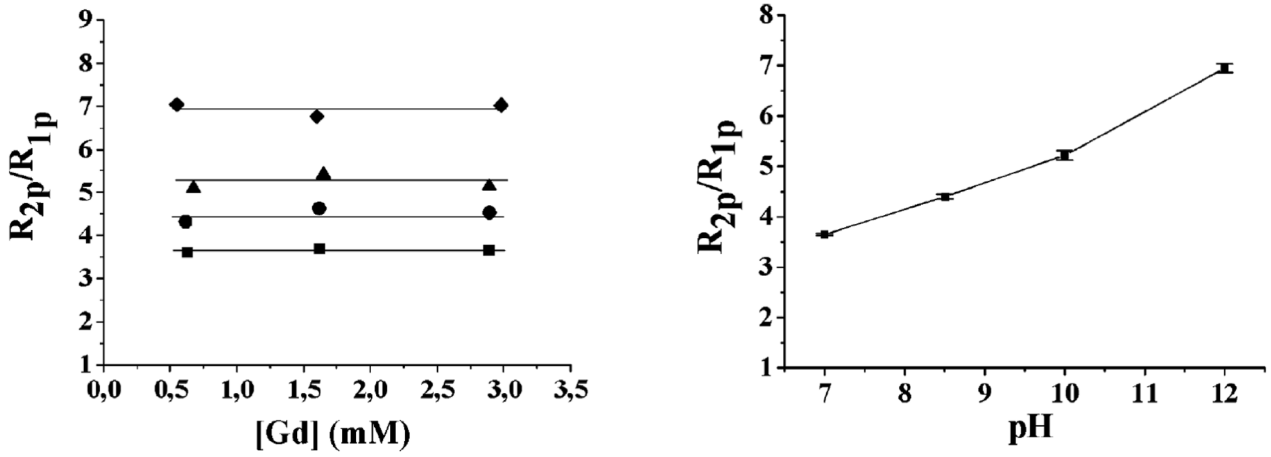

Fig. 5. (Left) Dependence of the relaxometric ratio on the concentration of Gd(III) for Gd-2 [(Gd-DOTAam)$_{33}$ Orn$_{205}$] at four pH values: pH 7 (squares), pH 8.5 (circles), pH 10 (triangles), and pH 12 (diamonds) (600 MHz, 25°C). (Right) Corresponding pH dependence of the relaxometric ratio calculated using the data points reported on the left. Adapted from Aime et al. (31) with permission of American Chemical Society.

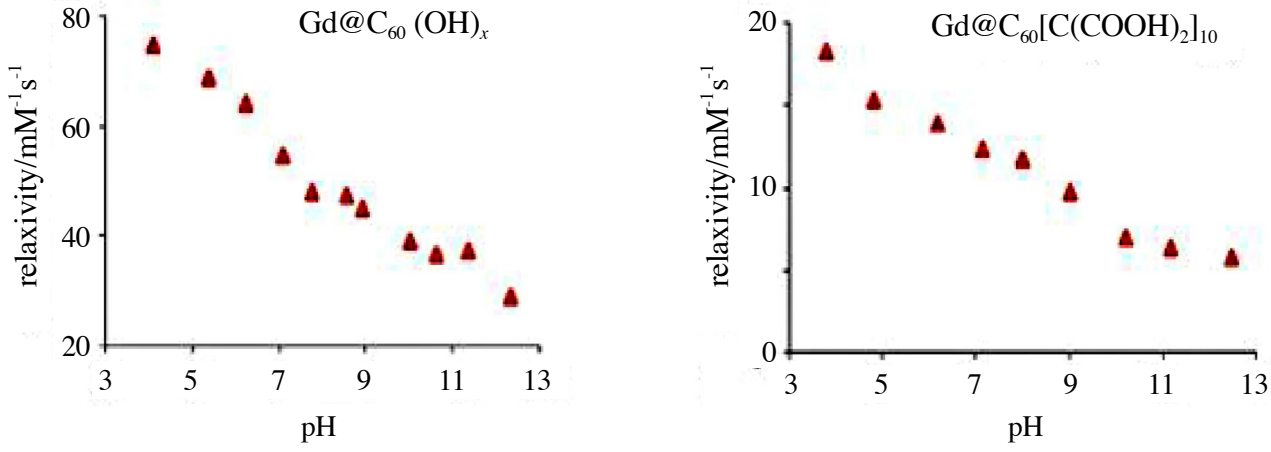

Fig. 6. pH dependency of the proton relaxivities for Gd@C_{60} $(OH)_x$ (left) and Gd@$C_{60}[(COOH)_2]_{10}$ (right) at 60 MHz and 26.1°C. Adapted from Toth et al. (32) with permission of American Chemical Society.

motion to minimize the relaxivity. We reported Gd-based MR contrast agents with uridine conjugation (33). The self-assembled contrast agent Gd-2 (LGd3) showed pH-dependent changes in relaxivity, probably due to the changes in aggregation and proton exchange rate (Fig. 7) of water in variable pH- buffer solution.

Further, Woods et al. (34) have developed a new Gd^{3+}-based contrast agent with p-nitrophenolic pendant arm Gd-3 (NP-DO3A; 2,2',2''-(10-(2-hydroxy-5-nitrobenzyl)-1,4,7,10-tetraazacyclododecane-1,4,7-triyl)triacetic acid). The study investigated the effect of pH on relaxivity at 20 MHz and 25°C. The relaxivity of the contrast agent Gd-3 was gradually reduced with increasing pH; however, the amide form of Gd-3 (NP-DO3AM; 2,2',2''-(10-(2-hydroxy-5-nitrobenzyl)-1,4,7,10-tetraazacyclododecane-1,4,7-triyl) triacetamide) failed to show such pH-dependent variation (Fig. 8). The relaxivity (r1) of Gd-3 (NP-DO3A) at pH4 was the highest (7.0 $mM^{-1}s^{-1}$), which was similar to the hydration number 2 in case of Gd(DO3A) (6.9 $mM^{-1}s^{-1}$). By contrast, at higher pH (8.5) the relaxivity of Gd-3 declined to 4.1 $mM^{-1}s^{-1}$, which was similar to DOTA with a hydration number 1. Such pH-dependent relaxivity changes in Gd-3 were attributed to the phenolic proton transfer, following ionization at higher pH resulting in induction of negative charge density on the metal ion complex. Most importantly, this contrast agent was stable against endogenous anionic species and Zn^{2+} ion.

Frullano et al. (35) have reported the development of a Gd-DOTA-based MR contrast agent with non-coordinated extended phosphonate functionality along with a PET-responsive ^{19}F unit. The contrast agent Gd-DOTA-4AMP-F facilitated pH estimation via T_1-W MRI and PET. Later, the

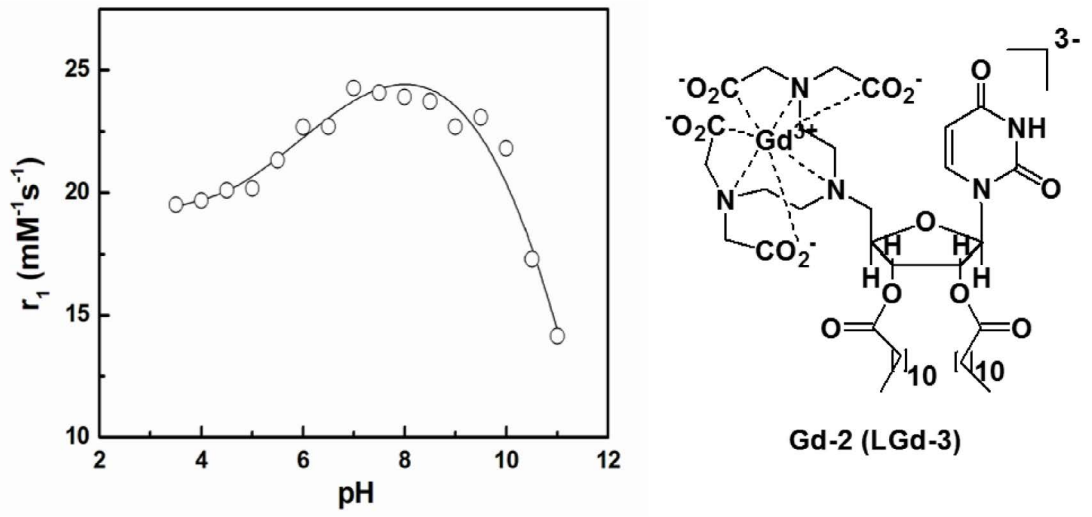

Fig. 7. pH dependency of proton relaxivity of Gd-2 (Lgd-3) at 60 MHz and 25.0°C. Adapted from Bhuniya et al. (33), with permission of Elsevier.

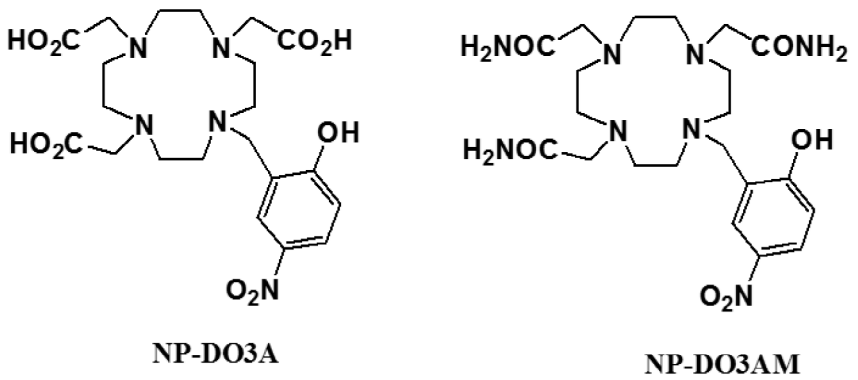

Fig. 8. Structure of Gd-3 (NP-DO3A) and NP-DO3AM. Adapted from Woods et al. (34), with permission of American Chemical Society.

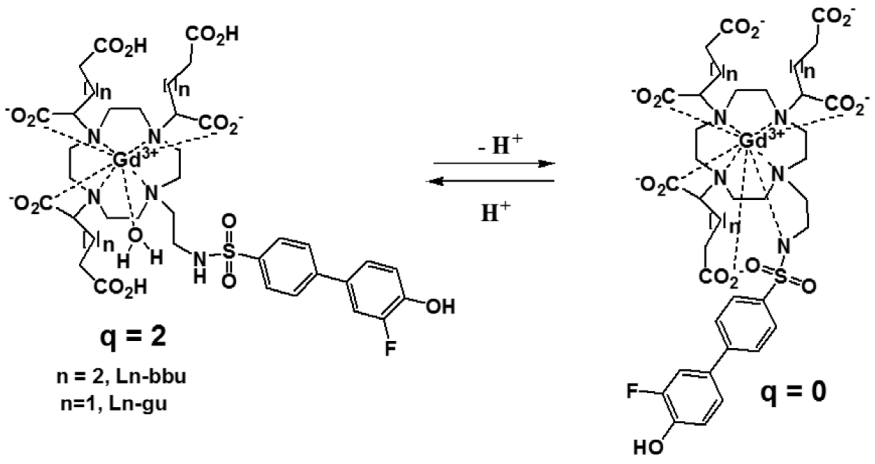

Fig. 9. Chemical structure of pH-dependent MR contrast agents (35). Adapted from Moriggi et al. (36) with permission of Wiley.

same group developed two new sulfonamide-conjugated contrast agents (Fig. 9), which exhibited changes in relaxivity because of the increases in hydration number from 0 to 2 at lower pH. Unfortunately, such probes are not stable under biological conditions due to the instability of Gd-complex (36).

Kim and his group (37) have developed pH-responsive micelles in which PEG-p(L-LA)-DTPA-Gd was encapsulated by pH-responsive oligomer PEG-p(L-His). At physiological pH, the stable self-assembled micelle resulted in low T_1 relaxivity due to the lower population of the water molecules in the primary coordination sphere. On the other hand, the low pH in the tumor microenvironment facilitated protonation of histidine residue in PEG-p(L-His). Thus, the micelle was dissembled, which increased the water molecule population in the primary coordination sphere; subsequently, the T_1 relaxivity was increased multifold. The new strategic contrast agent allowed detection of tumors measuring 3 mm^3 with a low diameter. Such strategy prompted the development of new contrast agents that were potentially successful in clinical trials.

In conclusion, we discussed the recent development of pH-driven Gd^{3+}-chelated T_1 MR contrast agents. Cyclen-based contrast agents have been designed for pH assessment. Uncoordinated phosphonate-based and dendrimer contrast agents were used in small animal models to map pH fluctuation in kidneys and tumors. Manipulation of parameters, such as aggregation-induced changes in relaxivity, as well as changes in water proton exchange rate and hydration number in the primary coordination sphere led to the development of pH-responsive contrast agents. However, the variation in pH-dependent hydration number does not have any real-world application as such contrast agents are unstable under physiological conditions. The local concentrations of Gd^{3+} chelator play a significant role in contrast enhancement. Therefore, the development of Gd^{3+}-based agents with the potential to estimate proton density (pH) in disease states, is a challenge. As MRI is the most preferable noninvasive tool for diagnosis, a new set of contrast agents will be developed to overcome the limitations associated with the present contrast agent.

Acknowledgments

This work was supported by the Brain Pool program funded by the Ministry of Science and ICT through the National Research Foundation of Korea (2018H1D3A2002203).

REFERENCES

1. Boron WF, Boulpaep EL. Medical physiology: a cellular and molecular approach. Philadelphia: Saunders/Elsevier, 2008
2. Lambers H, Piessens S, Bloem A, Pronk H, Finkel P. Natural skin surface pH is on average below 5, which is beneficial for its resident flora. Int J Cosmet Sci 2006;28:359-370
3. Han J, Burgess K. Fluorescent indicators for intracellular pH. Chem Rev 2010;110:2709-2728
4. Adrogué HJ, Wesson DE. Overview of acid base disorders. In: Adrogué HJ, Wesson DE, eds. Blackwell's basics of medicine. Acid-base. Boston: Blackwell Science, 1994;49-133
5. Vander Heiden MG, Cantley LC, Thompson CB. Understanding the Warburg effect: the metabolic requirements of cell proliferation. Science 2009;324:1029-

1033
6. Behne MJ, Barry NP, Hanson KM, et al. Neonatal development of the stratum corneum pH gradient: localization and mechanisms leading to emergence of optimal barrier function. J Invest Dermatol 2003;120:998-1006
7. Ilic D, Mao-Qiang M, Crumrine D, et al. Focal adhesion kinase controls pH-dependent epidermal barrier homeostasis by regulating actin-directed Na+/H+ exchanger 1 plasma membrane localization. Am J Pathol 2007;170:2055-2067
8. Okabe Y, Medzhitov R. Tissue-specific signals control reversible program of localization and functional polarization of macrophages. Cell 2014;157:832-844
9. Lee MH, Park N, Yi C, et al. Mitochondria-immobilized pH-sensitive off-on fluorescent probe. J Am Chem Soc 2014;136:14136-14142
10. Chen G, Fu Q, Yu F, et al. Wide-acidity-range pH fluorescence probes for evaluation of acidification in mitochondria and digestive tract mucosa. Anal Chem 2017;89:8509-8516
11. Podder A, Won M, Kim S, et al. A two-photon fluorescent probe records the intracellular pH through 'OR' logic operation via internal calibration. Sensors and Actuators B: Chemical 2018;268:195-204
12. Raghunand N, Altbach MI, van Sluis R, et al. Plasmalemmal pH-gradients in drug-sensitive and drug-resistant MCF-7 human breast carcinoma xenografts measured by 31P magnetic resonance spectroscopy. Biochem Pharmacol 1999;57:309-312
13. Mason RP. Transmembrane pH gradients in vivo: measurements using fluorinated vitamin B6 derivatives. Curr Med Chem 1999;6:481-499
14. Ojugo AS, McSheehy PM, McIntyre DJ, et al. Measurement of the extracellular pH of solid tumours in mice by magnetic resonance spectroscopy: a comparison of exogenous (19)F and (31)P probes. NMR Biomed 1999;12:495-504
15. van Sluis R, Bhujwalla ZM, Raghunand N, et al. In vivo imaging of extracellular pH using 1H MRSI. Magn Reson Med 1999;41:743-750
16. Garcia-Martin ML, Herigault G, Remy C, et al. Mapping extracellular pH in rat brain gliomas in vivo by 1H magnetic resonance spectroscopic imaging: comparison with maps of metabolites. Cancer Res 2001;61:6524-6531
17. Vermathen P, Capizzano AA, Maudsley AA. Administration and (1)H MRS detection of histidine in human brain: application to in vivo pH measurement. Magn Reson Med 2000;43:665-675
18. Mori S, Eleff SM, Pilatus U, Mori N, van Zijl PC. Proton NMR spectroscopy of solvent-saturable resonances: a new approach to study pH effects in situ. Magn Reson Med 1998;40:36-42
19. Ward KM, Balaban RS. Determination of pH using water protons and chemical exchange dependent saturation transfer (CEST). Magn Reson Med 2000;44:799-802
20. Goldman MR, Brady TJ, Pykett IL, et al. Quantification of experimental myocardial infarction using nuclear magnetic resonance imaging and paramagnetic ion contrast enhancement in excised canine hearts. Circulation 1982;66:1012-1016
21. Caravan P. Strategies for increasing the sensitivity of gadolinium based MRI contrast agents. Chem Soc Rev 2006;35:512-523
22. Koenig SH. A novel derivation of the Solomon-Bloembergen-Morgan equations: application to solvent relaxation by Mn2+-protein complexes. J Magn Reson 1978;31:1-10
23. Westlund PO. A generalized Solomon-Bloembergen-Morgan theory for arbitrary electron spin quantum number S - the dipole-dipole coupling between a nuclear spin I = 1/2 and an electron spin system S = 5/2. Mol Phys 1995;85:1165-1178
24. Kowalewski J, Luchinat C, Nilsson T, Parigi G. Nuclear spin relaxation in paramagnetic systems: electron spin relaxation effects under near-red field limit conditions and beyond. J Phys Chem A 2002;106:7376-7382
25. Yin J, Chen D, Zhang Y, Li C, Liu L, Shao Y. MRI relaxivity enhancement of gadolinium oxide nanoshells with a controllable shell thickness. Phys Chem Chem Phys 2018;20:10038-10047
26. Zech SG, Eldredge HB, Lowe MP, Caravan P. Protein binding to lanthanide(III) complexes can reduce the water exchange rate at the lanthanide. Inorg Chem 2007;46:3576-3584
27. Werner EJ, Datta A, Jocher CJ, Raymond KN. High-relaxivity MRI contrast agents: where coordination chemistry meets medical imaging. Angew Chem Int Ed Engl 2008;47:8568-8580
28. Zhang S, Wu K, Sherry AD. A novel pH-Sensitive MRI contrast agent. Angew Chem Int Ed Engl 1999;38:3192-3194
29. Ali MM, Woods M, Caravan P, et al. Synthesis and relaxometric studies of a dendrimer-based pH-responsive MRI contrast agent. Chemistry 2008;14:7250-7258
30. Garcia-Martin ML, Martinez GV, Raghunand N, Sherry AD, Zhang S, Gillies RJ. High resolution pH(e) imaging of rat glioma using pH-dependent relaxivity. Magn Reson Med 2006;55:309-315
31. Aime S, Fedeli F, Sanino A, Terreno E. A R2/R1 ratiometric procedure for a concentration-independent, pH-responsive, Gd(III)-based MRI agent. J Am Chem Soc 2006;128:11326-

11327

32. Toth E, Bolskar RD, Borel A, et al. Water-soluble gadofullerenes: toward high-relaxivity, pH-responsive MRI contrast agents. J Am Chem Soc 2005;127:799-805
33. Bhuniya S, Moon H, Lee H, et al. Uridine-based paramagnetic supramolecular nanoaggregate with high relaxivity capable of detecting primitive liver tumor lesions. Biomaterials 2011;32:6533-6540
34. Woods M, Kiefer GE, Bott S, et al. Synthesis, relaxometric and photophysical properties of a new pH-responsive MRI contrast agent: the effect of other ligating groups on dissociation of a p-nitrophenolic pendant arm. J Am Chem Soc 2004;126:9248-9256
35. Frullano L, Catana C, Benner T, Sherry AD, Caravan P. Bimodal MR-PET agent for quantitative pH imaging. Angew Chem Int Ed Engl 2010;49:2382-2384
36. Moriggi L, Yaseen MA, Helm L, Caravan P. Serum albumin targeted, pH-dependent magnetic resonance relaxation agents. Chemistry 2012;18:3675-3686
37. Kim KS, Park W, Hu J, Bae YH, Na K. A cancer-recognizable MRI contrast agents using pH-responsive polymeric micelle. Biomaterials 2014;35:337-343